**International Conference on Space Optics—ICSO 2018**

Chania, Greece

9–12 October 2018

*Edited by Zoran Sodnik, Nikos Karafolas, and Bruno Cugny*


# *An adaptive coded transmission scheme utilizing frozen bits of polar code in satellite laser communications*


*K. Ito*

*E. Okamoto*

*H. Kunimori*

*M. Toyoshima*



International Conference on Space Optics — ICSO 2018, edited by Zoran Sodnik, Nikos Karafolas, Bruno Cugny, Proc. of SPIE Vol. 11180, 111805Y · © 2018 ESA and CNES · CCC code: 0277-786X/18/$18 · doi: 10.1117/12.2536133

# An Adaptive Coded Transmission Scheme Utilizing Frozen Bits of Polar Code in Satellite Laser Communications

K. Ito[a], E. Okamoto[a], H. Takenaka[b], H. Kunimori[b], and M. Toyoshima[b]
[a]Graduate School of Engineering, Nagoya Institute of Technology
Gokiso-cho, Showa-ku, Nagoya, Aichi 466-855, Japan.
[b]National Institute of Information and Communications Technology
Nukui-Kitamachi, Koganei, Tokyo, 184-8795, Japan.

## ABSTRACT

Free-space optical communication for a satellite-to-ground link using wideband 10-THz lasers can realize a higher capacity than radio frequency (RF) communications, and use downsized and energy-efficient components. Thus, satellite laser communication is expected to be used in new communication infrastructures. However, in wireless optical communication, problems such as disturbances due to atmospheric fluctuation and tracking/capturing errors of the laser beam occur, leading to a reduction in the received optical power. Thus, powerful channel coding is essential. On the other hand, it is strictly proven that polar code asymptotically reaches the channel capacity with sufficiently long code length. To obtain the excellent decoding characteristics of the polar code, it is necessary to adequately set frozen bits that are shared by the transmitter and the receiver, and an arbitrary code rate can easily be achieved by controlling the number of frozen bits. However, when considering the application of adaptive polar code to satellite laser communications, there are some difficulties in the transmission link such as large delays or received power fluctuation caused by air turbulence. Thus, it is difficult to realize an adaptive coding scheme for the channel with two-way information control. Therefore, in this paper, we propose a one-way adaptive polar coding scheme that estimates the transmission rate without requiring control information by superimposing code rate information into frozen bits, and estimating the code rate by decoding them at the receiver side. We evaluate the characteristics of this method using computer simulations.

**Keywords:** polar code, successive cancellation list decoding, adaptive coding, satellite laser communication

## 1. INTRODUCTION

In recent years, the demand for higher capacity terrestrial wireless communication has increased because of the widespread use of mobile terminals. Similarly, in satellite communications, the demand for a large communication capacity has been progressively increasing because of the performance improvement of sensors and cameras. Currently, satellite RF communications are mainly used. However, high capacity transmission (i.e., over 10 Gbps) is difficult in satellite RF communication due to the bandwidth limitation. As an alternative, free space optics in satellite communications are attracting much attention [1]. Because the laser light of the 10-THz band is used for the communication medium, it is possible not only to greatly increase the communication capacity, but also to downsize and increase the power savings of the apparatus. Furthermore, because the laser light has strong directivity and uses a very narrow beam, there are fewer possibilities of eavesdropping and interference. However, because of the directivity of the laser beam, highly accurate pointing and tracking mechanisms are necessary at both the transmitter and the receiver. In the satellite laser transmission, received power loss occurs because of this tracking error, in addition to air turbulence between ground and satellite terminals. Therefore, forward error correction technology with powerful error correction is indispensable. In 2014, satellite laser communication at 10 Mbps was achieved between the Space Optical Communications Research Advanced Technology Satellite (SOCRATES), a small satellite equipped with a small optical transponder (SOTA), and the ground station [2] with using low density generator matrix (LDGM) code [3].

On the other hand, polar code is a kind of linear channel code proposed by E. Arıkan in 2008 [4]. It is strictly proven that polar code with a code length $N$ asymptotically approaches the channel capacity, in which the decoding complexity is relatively low in $O(N \log N)$. It has recently been reported that polar code using successive cancellation list decoding (SCLD) [5] with cyclic redundancy check (CRC) code at a relatively short code length outperforms turbo code [6] and

LDPC code [7]. To obtain this strong error correcting ability, it is necessary to appropriately set frozen bits, which are dummy bits whose positions in a codeword are shared with the transmitter and the receiver. In polar code, arbitrary code rates can be composed by changing the number of frozen bits. When using the adaptive coding with polar code, the number of frozen bits becomes side information that should be negotiated between the transmitter and the receiver. However, because of the large delay and the received-power fluctuations, advanced two-way control for adaptive coding based on the instantaneous channel state is difficult to implement in satellite laser communication. Here, we found that one-way adaptive polar coding can be composed if the coding rate index is embedded in some of the frozen bits [8]. In this scheme, rate estimation and decoding can be simultaneously performed at the receiver. However, our previous study considered a terrestrial channel, and thus, the performance of a satellite laser channel was not considered.

Therefore, in this paper, we propose a one-way adaptive polar coding scheme for satellite laser communication in which the coding rate information is embedded in a section of frozen bits; the rate estimation and decoding at the receiver are conducted using SCLD. The performance of the proposed scheme is evaluated using numerical simulations.

In the following section, the structure of polar code is reviewed. The proposed one-way adaptive polar coding scheme is introduced in Section 3. The numerical results are given in Section 4. Conclusions are given in Section 5.

## 2. POLAR CODE

### 2.1 Construction of polar code

In what follows, the vector consisting of $(a_0, a_1, \dots, a_{N-1})$ is denoted by $\mathbf{a}_0^{N-1}$, and let the $(i, j)$ component of matrix **A** be $a_{i,j}$. To generate the codeword for polar code, we use a generator matrix with a size that is an integer power of 2. Here, if the code length $N$ is set to $N = 2^n$, the generator matrix $\mathbf{G}_N$ can be calculated recursively by

$$\mathbf{G}_N = (\mathbf{I}_N \otimes \mathbf{G}_2)\mathbf{R}_N(\mathbf{I}_2 \otimes \mathbf{G}_{N/2}) \tag{1}$$

where $\mathbf{I}_N$ is an $N \times N$ unit matrix, the initial matrix $\mathbf{G}_2$ is $\mathbf{G}_2 = \begin{bmatrix} 1 & 0 \\ 1 & 1 \end{bmatrix}$, and $\mathbf{R}_N$ is an $N \times N$ substitution matrix called the reverse-shuffle matrix, which is defined by

$$(x_0, x_1, \dots, x_{N-1})\mathbf{R}_N = (x_0, x_2, \dots, x_{N-2}, x_1, x_3, \dots x_{N-1}) \tag{2}$$

Moreover, $\otimes$ denotes the Kronecker product. Here, if $p \times q$ matrix **A** and $s \times t$ matrix **B** are given, then the Kronecker product of **A** and **B** is given by

$$\mathbf{A} \otimes \mathbf{B} = \begin{bmatrix} a_{0,0}\mathbf{B} & \cdots & a_{1,q-1}\mathbf{B} \\ \vdots & \ddots & \vdots \\ a_{p-1,0}\mathbf{B} & \cdots & a_{p-1,q-1}\mathbf{B} \end{bmatrix} \tag{3}$$

Then, the polar codeword $\mathbf{x}_0^{N-1}$, $x_i \in \{0, 1\}$ is obtained using $\mathbf{G}_N$ from the information sequence $\mathbf{u}_0^{N-1}$, $\mathrm{u} \in \{0, 1\}$ via the following equation.

$$\mathbf{x}_0^{N-1} = \mathbf{u}_0^{N-1}\mathbf{G}_N \tag{4}$$

The encoder structure corresponding to $\mathbf{G}_N$ $(N = 8)$ is shown in Figure 1.

In polar code, the channel capacity of the communication path $\mathbf{W}_n = \left\{W_n^{(i)} \mid i = 0, 1, \dots, N-1\right\}$ corresponding to information bits $\mathbf{u}_0^{N-1}$ is polarized to 0 or 1; this method is called channel polarization. When the information bits are not assigned in $W_n^{(i)}$, with a low capacity close to 0, an arbitrary channel coding rate can be easily constructed by changing the number of unassigned bits. These bits are called frozen bits and are shared between the transmitter and the receiver. Assuming an information bit length $K$ and a frozen bit length $(N - K)$, the coding rate $R$ becomes $R = K/N$. Various methods of determining the frozen bits have been proposed [4, 9, 10]. In the determination method using the Bhattacharya parameter [9], the communication paths $\mathbf{W}_0^{N-1}: \mathbf{x}_0^{N-1} \rightarrow \boldsymbol{y}_0^{N-1}$ are assumed to be binary erasure channels, and frozen bits are decided based on the upper bound of the error probability of each bit. In the Monte-Carlo method, frozen bits are decided based on the error rate of each bit, which is calculated by a computer simulation in advance [10].

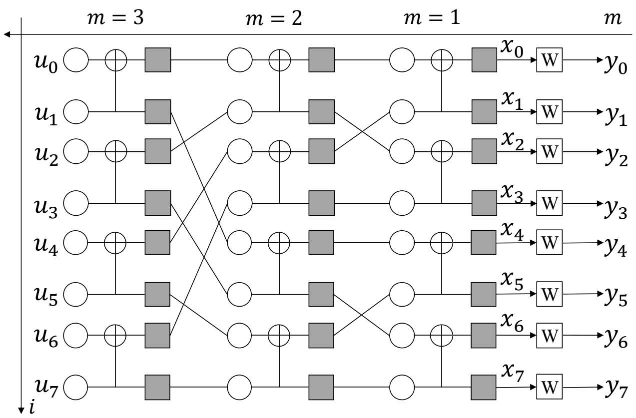


Figure 1. Construction of polar encoder $\mathbf{G}_N$ $(\boldsymbol{N}=\mathbf{8})$.

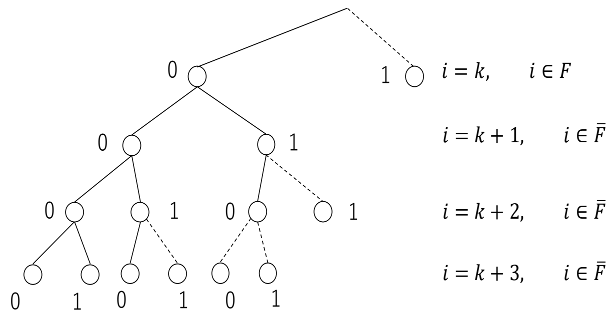


Figure 2. Schematic diagram of SCLD at $\boldsymbol{L_{max}}=\mathbf{3}$.

## 2.2 Successive cancellation list decoding

We first introduce successive cancellation decoding (SCD), which is the basis of SCLD. SCD is a decoding method using polar code [4]. In SCD, it is assumed that decoding until $(i-1)$ bits of $\mathbf{u}_0^{N-1}$ is successful, and that $\hat{u}_i$ decoding is sequentially conducted from $i=0$. The decoding calculation is performed based on the log likelihood ratio (LLR), and the LLR of $L_\lambda^{(\phi)}$ can be recursively calculated using the following equation [10].

$$L_\lambda^{(2\phi)}=f_u\left(L_{\lambda-1}^{(2\phi-[\phi\ mod\ 2^{\lambda-1}])},L_{\lambda-1}^{(2^\lambda+2\phi-[\phi\ mod\ 2^{\lambda-1}])}\right) \tag{5}$$

$$L_\lambda^{(2\phi+1)}=f_l\left(L_{\lambda-1}^{(2\phi-[\phi\ mod\ 2^{\lambda-1}])},L_{\lambda-1}^{(2^\lambda+2\phi-[\phi\ mod\ 2^{\lambda-1}])},\mathbf{u}_{0,e}^{2i}\oplus\mathbf{u}_{0,o}^{2i}\right) \tag{6}$$

where $\phi$ and $\lambda$ satisfy $0\le\phi\le 2^\lambda$ and $0\le\lambda\le n$, respectively. $\mathbf{u}_{0,e}^{2i}$ and $\mathbf{u}_{0,o}^{2i}$ indicate the even- and odd-numbered elements of $\mathbf{u}_0^{2i}$, respectively, and $f_u, f_l$ are defined by the following equations.

$$f_u(\alpha,\beta)\triangleq 2\tanh^{-1}\left(\tanh\frac{\alpha}{2}\times\tanh\frac{\beta}{2}\right) \tag{7}$$

$$f_l(\alpha,\beta,u)\triangleq(-1)^u\alpha+\beta \tag{8}$$

Moreover, the initial value $L_0^{(i)}$ $(i=0,1,\dots,N-1)$ is obtained using the following equation using codeword $x_i$ and received value $y_i$.

$$L_0^{(i)}=\frac{\log_2 p(y_i|x_i=0)}{\log_2 p(y_i|x_i=1)} \tag{9}$$

where $p(y_i|x_i=b)$ represents the conditional probability that $y_i$ is received when the transmit bit is $b=\{0,1\}$. Then, based on the $L_n^{(\phi)}$ calculated using (5) to (8), the decision is made according to equation (10) to obtain the decoding result $\hat{u}_i$

$$\hat{u}_\mathrm{i}=\begin{cases}u_\mathrm{i} & \text{if } i\in F\\ 0 & \text{if } i\in\bar{F}, L_n^{(i)}\ge 0\\ 1 & \text{if } i\in\bar{F}, L_n^{(\mathrm{i})}<0\end{cases} \tag{10}$$

where $F$ is a set of frozen bits known to the receiver in advance.

On the other hand, in SCLD [5], the decoder preserves the decoding candidates up to the list size of $L_{max}$ in the process of SCD, according to the $L_{max}$ maximum LLRs, which are equivalent to minimum path metrics. Figure 2 shows an example of SCLD decoding. The path metric $PM_l^{(i)}$ for the $i$-th bit in path $l$ is calculated by

$$PM_l^{(i)}\triangleq\sum_{j=0}^{i}\ln\left(1+e^{(2\hat{u}_j[l]-1)\cdot L_n^{(j)}[l]}\right) \tag{11}$$

where $\hat{u}_j[l]$ and $L_n^{(j)}[l]$ are the decoded bit $\hat{u}_j$ and LLR $L_n^{(j)}$ in the $l$-th path, respectively. The selection of surviving paths is performed for increasingly smaller values of $PM_l^{(i)}$. In Figure 2, three paths are selected and stored using $PM_l^{(i)}$ [11].

## 3. PROPOSED ADAPTIVE CODING SCHEME

As described above, the encoding gain of polar code is obtained by utilizing the frozen bits known to both the transmitter and the receiver. Exploiting the frozen bits, a one-way adaptive multi-rate polar code transmission method without two-way control can be devised. In this method, the rate information is embedded in the frozen bits [8]. To simplify the study, we consider a two-mode adaptive downlink transmission method in what follows. At the transmitter, the following process is conducted.

1) The transmitter determines the appropriate code rate based on information at the transmitter side such as the predicated signal to noise ratio (SNR) at the receiver calculated from the satellite orbit or the required quality of services (QoS) of data to be transmitted. Here, the two rates are denoted as $R_1$ and $R_2$.

2) $\varepsilon$ bits in $\mathbf{u}_0^{N-1}$ are used for the mode index. This index is called the rate estimation bit hereafter; the rate estimation bits are determined for the selected mode. The Hamming distance of rate estimation bits should be enhanced, e.g., if $\varepsilon = 3$, code (000) and code (111) are used, etc.

3) In $\mathbf{u}_0^{N-1}$, the rate estimation bits are assigned first, so as to be correctly decoded by the receiver, at the $i$-th position that has sufficiently good capacity in $W_n^{(i)}$. Then, $K$ data bits are assigned to the remaining $(N-\varepsilon)$ bit positions.

4) Finally, the remaining $(N-K-\varepsilon)$ bits are set to 0 (i.e., as frozen bits). Thus, there are two types of $\mathbf{u}_0^{N-1}$ of $R_1$ and $R_2$, and it is assumed that the positions of frozen bits including $\varepsilon$ bits in $R_1$ and $R_2$ codes are shared at the receiver. Thus, the $(N-K)$ frozen bits are determined by embedding the rate information, and $K$ bits can be transmitted in both $R_1$ and $R_2$ polar codes as $K_1$ and $K_2$. Figure 3 shows the bit design of the proposed adaptive polar code. The rate estimation bits are inserted among the information bits and $\varepsilon$ bits of frozen bits are alternately used as the information bits. At the transmitter, the codeword $\mathbf{x}_0^{N-1}$ is obtained by encoding $\mathbf{u}_0^{N-1}$, and $\mathbf{x}_0^{N-1}$ is transmitted after being modulated.

At the receiver, rate estimation and decoding are jointly conducted. Let $\mathbf{y}_0^{N-1}$ be the received codeword through the channel when $\mathbf{x}_0^{N-1}$ is transmitted. The receiver first assumes either of the transmitted rates $R_1$ or $R_2$, and decoding is conducted based on the assumed rate. In SCLD decoding, (5) to (10) are conducted, where in the bit detection of (10), the index bits are used for rate estimation bits in the frozen bits. Then, the LLRs of the quasi-maximum likelihood and sequence estimation for $R_1$ and $R_2$ are obtained. Finally, the coding rate is determined using the LLRs. In particular, the path metric of each rate $R_k$ $(k = 1.2)$ is calculated by

$$PM_e^{(R_k)} = \sum_{i \in \mathbf{E}} \ln\left(1 + \exp\left(-\left(1 - 2\hat{u}_i^{(R_k)}\right) L_i^{(R_k)}\right)\right) \tag{12}$$

where $\mathbf{E}$ is the position of rate estimation bits, and $\hat{u}_i^{(R_k)}$ and $L_i^{(R_k)}$ are the decoded bit $\hat{u}_i$ and LLR $L_i$ at rate $R_k$, respectively. Then, the $R_k$ value with smaller $PM_e^{(R_k)}$ is selected as the transmitted mode.

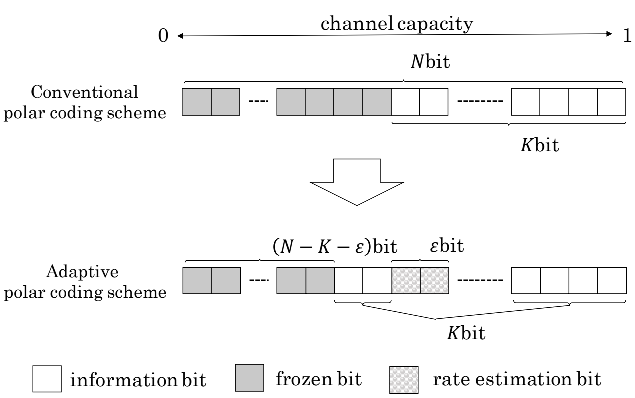


Figure 3. Frozen bit design of adaptive coded polar code.

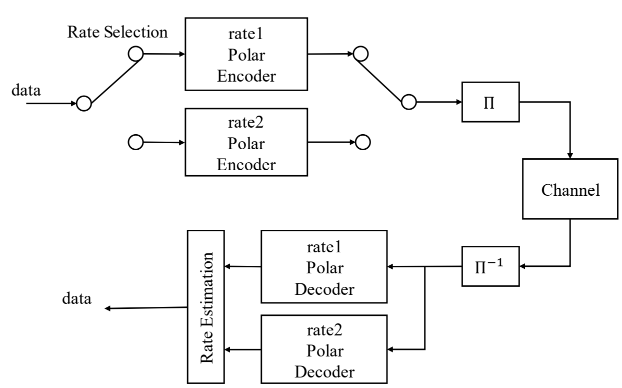


Figure 4. Block diagram of proposed system.

Table. 1 Simulation parameters.

| | Multi-rate adaptive polar code |
|---|---|
| Transmission direction | Forward link |
| Code length | $N = 2048$ |
| Code rate | 1/2, 1/8 |
| Frozen bit determination scheme | Modified Monte-Carlo method [11] |
| Modulation | BPSK |
| Channel | Atmospheric fluctuation with AWGN |
| Intensity variation probability distribution | Time correlated gamma-gamma distribution |
| Sampling time $\boldsymbol{\Delta t}$ [s] | $\mathbf{1.0 \times 10^{-6}}$ |
| Correlation time $\boldsymbol{\tau_c}$ [s] | $\mathbf{1.0 \times 10^{-3}}$ |
| Scintillation index (SI) | 0.2 |
| Channel state information | Perfect |
| Interleaver | S random Interleaver, $\boldsymbol{S = 20}$ |
| Decoding scheme | Successive cancellation list decoding |

## 4. NUMERICAL RESULTS

We calculated the characteristics of the proposed adaptive polar code and compared it to the conventional single-rate polar code using computer simulations. Figure 4 shows the system block diagram of the proposed adaptive polar code transmission method. Table 1 shows the simulation parameters. Frozen bits for each rate are determined using the modified Monte-Carlo method [12], where the frozen bits are selected by the advanced bit error rate calculation, whereas the frozen bit order is uniquely determined from a frozen bit vector to be applied to any code rates. $\varepsilon = 3$ is used, as (000) and (111) are used for $R_1$ and $R_2$, respectively. The satellite laser channel fluctuates because of air scintillation and pointing/tracking errors, resulting in a burst error. This channel is modeled as a time-correlated gamma-gamma disturbance channel [13, 14]. Therefore, we assume a gamma-gamma distribution channel based on the Bykhovsky formula [15].

First, we evaluate the rate estimation performance at the receiver. Figures 5 and 6 show the block error rate (BLER) of the proposed method with single-rate polar code, and the rate estimation error rate, respectively. Here, the rate of the proposed method is fixed at 1/2 or 1/8, and the decoding performance is evaluated. Figure 5 confirms that almost the same BLER is obtained using the proposed method for single-rate transmission. In Figure 6, the rate estimation error occurs in the low SNR region only when 1/2 code is transmitted, because of the relatively high code rate. However, the degradation is negligible, as shown in Figure 5.

Next, Figure 7 shows the throughput characteristics of the proposed method, where the transmission rate is adaptively selected based on the estimated receiver SNR calculated based on satellite orbit, etc. At the receiver, the joint rate estimation and decoding described in Section 3 is conducted. The results show that the proposed scheme can achieve the higher throughput of two single-rate transmissions. Therefore, one-way multi-rate transmission of polar code could be realized.

## 5. CONCLUSIONS

In this paper, we proposed an adaptive channel coding scheme using polar code and SCLD for satellite laser communications; results showed good performances in terms of BLER, rate estimation error, and throughput in the satellite-to-ground channel. In the proposed scheme, by embedding the rate estimation bits into the polar codeword, whose frozen bit patterns are shared between the transmitter and the receiver, one-way adaptive transmission can be realized. At the receiver, joint rate estimation and decoding are conducted based on the received codeword. Using this scheme, adaptive polar code transmission that can follow the predicted receiver SNR, data QoS, or data queue is realized.

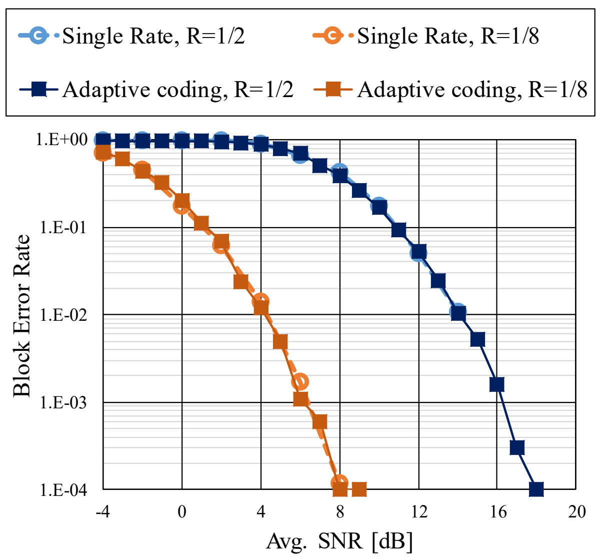


Figure 5. Comparison of block error rate for adaptive single-rate polar codes.

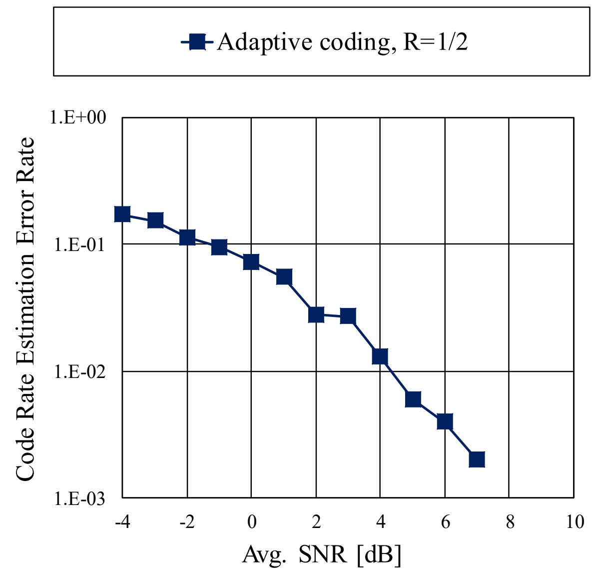


Figure 6. Rate estimation error performance for adaptive polar code.

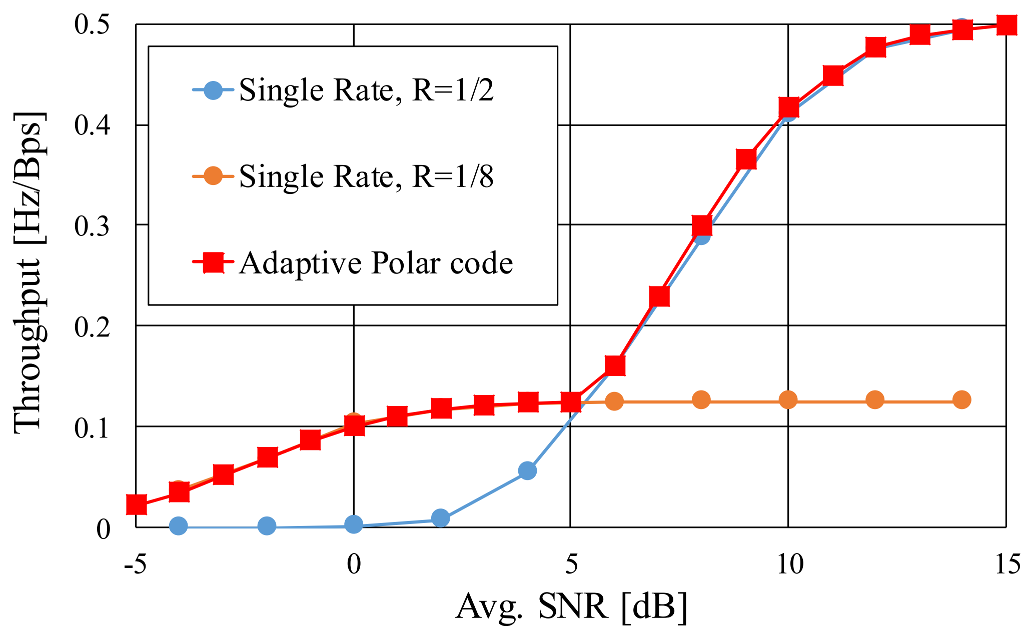


Figure 7. Comparison of throughput for adaptive or single-rate polar code.

## REFERENCES

[1] Fuse T., Akioka M., Kolev D., Koyama Y., Kubo-oka T., Kunimori H., Suzuki K., Takenaka H., Munemasa Y., and Toyoshima M., "Development of a Breadboard Model of Space Laser Communication Terminal for Optical Feeder Links from Geo," Proc. SPIE International Conference on Space Optics (ICSO2016), 1-4, (2016).

[2] Phung D.-H., et al., "Telecom & Scintillation First Data Analysis for DOMINO – Laser Communication between SOTA, Onboard Socrates Satellite, and MEO OGS," Proc. IEEE ICSOS, 1-7, (2015).

[3] V. Roca and C. Neumann, "Design, Evaluation and Comparison of Four Large Block FEC Codecs, LDPC, LDGM, LDGM Staircase and LDGM Triangle, plus a Reed-Solomon Small Block FEC Codec," Res. Rep. 5225, INRIA, pp. 1–24, 2006.

[4] Arıkan E., "Channel Polarization: A Method for Constructing Capacity-Achieving Codes for Symmetric Binary-Input Memoryless Channels," IEEE Transactions on Information Theory, 55(7), 3051-3073, (2009).

[5] Tal I., Vardy A., "List Decoding of Polar Codes," Proc. IEEE Information Theory Society, 61(5), 2213-2226, (2015).

[6] Berrou C., et al., "Near Shannon Limit Error-correcting Coding and Decoding: Turbo-codes," Proc. IEEE Int'l Conf. on Commun. 93(2), 1064-1070, (1993).

[7] Niu K., Chen K., "CRC-Aided Decoding of Polar Codes," Proc. IEEE Communications Society, 16(10), 1089-77898, (2012).

[8] Ito K., Okamoto E., Takenaka H., Kunimori H., Toyoshima M., "A Study on Adaptive Coded Transmission Scheme using Polar Code," IEICE-RCS2017-282, 117(396), 79-83, (2018). (Japanese).

[9] Li H., Sun Y., "A Practical Construction Method for Polar Codes in AWGN Channels," Proc. IEEE Communications Letters, 18(11), 223-226, 2013.

[10] Trifonov P., "Efficient Design and Decoding of Polar Codes," Proc. IEEE Transactions on Communications, 60(11), 3221-3227, (2012).

[11] Stimming A. B., Parizi M. B., "LLR-Based Successive Cancellation List Decoding," Proc. IEEE Signal Processing Society, 63(19), 5165-5179, (2015).

[12] Watanabe Y., Suyama S., Nagata S., Miki N., "Frozen Bit Determination Method Based on Error Rate," IEICE-RCS2016-159, 116(257), 35-39, (2016). (Japanese).

[13] Anguita J., Djordjevic I., Neifeld M., and Vasic B., "Shannon Capacities and Error-correction Codes for Optical Atmospheric Turbulent Channels," J. Optical Networking, 4(9), 586-601, (2005).

[14] Al-Habash M. A., Andrews L. C., and Phillips R. L., "Mathematical Model for the Irradiance Probability Density Function of a Laser Beam Propagating through Turbulent Media," Journal of Optical Networking, 40(8), 1554-1562, (2001).

[15] Bykhovsky D., "Simple Generation of Gamma, Gamma–gamma, and K Distributions with Exponential Autocorrelation Function," Journal of Lightwave Technology, 34(9), 2106-2110, (2016).